



## 32 **Summary Paragraph**

33 The field of gene therapy has been galvanized by the discovery of the highly efficient and  
34 adaptable site-specific nuclease system CRISPR/Cas9 from bacteria.<sup>1,2</sup> Immunity against  
35 therapeutic gene vectors or gene-modifying cargo nullifies the effect of a possible curative  
36 treatment and may pose significant safety issues.<sup>3-5</sup> Immunocompetent mice treated with  
37 CRISPR/Cas9-encoding vectors exhibit humoral and cellular immune responses against the  
38 Cas9 protein, that impact the efficacy of treatment and can cause tissue damage.<sup>5,6</sup> Most  
39 applications aim to temporarily express the Cas9 nuclease in or deliver the protein directly into  
40 the target cell. Thus, a putative humoral antibody response may be negligible.<sup>5</sup> However,  
41 intracellular protein degradation processes lead to peptide presentation of Cas9 fragments on  
42 the cellular surface of gene-edited cells that may be recognized by T cells. While a primary T  
43 cell response could be prevented or delayed, a pre-existing memory would have major impact.  
44 Here, we show the presence of a ubiquitous memory/effector T cell response directed towards  
45 the most popular Cas9 homolog from *Streptococcus pyogenes* (SpCas9) within healthy human  
46 subjects. We have characterized SpCas9-reactive memory/effector T cells ( $T_{EFF}$ ) within the  
47 CD4/CD8 compartments for multi-effector potency and lineage determination. Intriguingly,  
48 SpCas9-specific regulatory T cells ( $T_{REG}$ ) profoundly contribute to the pre-existing SpCas9-  
49 directed T cell immunity. The frequency of SpCas9-reactive  $T_{REG}$  cells inversely correlates with  
50 the magnitude of the respective  $T_{EFF}$  response. SpCas9-specific  $T_{REG}$  may be harnessed to  
51 ensure the success of SpCas9-mediated gene therapy by combating undesired  $T_{EFF}$  response  
52 *in vivo*. Furthermore, the equilibrium of Cas9-specific  $T_{EFF}$  and  $T_{REG}$  cells may have greater  
53 importance in *Streptococcus pyogenes*-associated diseases. Our results shed light on the T  
54 cell mediated immunity towards the much-praised gene scissor SpCas9 and offer a possible  
55 solution to overcome the problem of pre-existing immunity.

## 56 **Text**

57 SpCas9 was the first Clustered Regularly Interspaced Short Palindromic Repeats (CRISPR)  
58 associated nuclease hijacked to introduce DNA double-strand breaks at specific DNA sequences.<sup>1</sup>  
59 Through the ease of target adaption and the remarkable efficacy, it advanced to the most popular  
60 tool for re-writing genes in research and potential clinical applications. The major concern for  
61 clinical translation of CRISPR/Cas9 technology is the risk for off-target activity causing potentially  
62 harmful mutations or chromosomal aberrations.<sup>2,7</sup> High-fidelity Cas9 enzymes were developed to  
63 reduce the probability of these events.<sup>8</sup> Furthermore, novel Cas9-based fusion proteins allow base  
64 editing or specific epigenetic reprogramming without inducing breaks in the DNA.<sup>9,10</sup> Most  
65 approaches are based on the original SpCas9 enzyme that originates in the facultatively

66 pathogenic bacterium *Streptococcus (S.) pyogenes*. Every eighth school-aged child has an  
67 asymptomatic colonization of the faucial mucosa.<sup>11</sup> *S. pyogenes*-associated pharyngitis and  
68 pyoderma are among the most common bacterial infection-related symptoms worldwide and can,  
69 sometimes lead to abysmal systemic complications.<sup>12</sup> Due to the high prevalence of *S. pyogenes*  
70 infections, we hypothesized that SpCas9 could elicit an adaptive memory immune response in  
71 humans. Very recently, SpCas9-reactive antibodies but not SpCas9-reactive T cells were detected  
72 in human samples.<sup>13</sup> The absence of detectable T cell reactivity in that study might be due to a  
73 sensitivity issue as only IFN- $\gamma$  expression was analysed. Anti-SpCas9-antibodies should not  
74 impact the success of gene therapy, since usually SpCas9 is either protected by a vector particle  
75 or directly delivered into the targeted cells. In contrast, a pre-existing T cell immunity, particularly  
76 if tissue-migrating T<sub>EFF</sub> cells are present, would result in a fast inflammatory and cytotoxic  
77 response to cells presenting Cas9 peptides on their major histocompatibility complexes (MHC)-  
78 molecules during or after intra-tissue gene editing.<sup>4</sup>

79 For detection of a putative SpCas9-directed T cell response, we stimulated human peripheral  
80 blood mononuclear cells (PBMCs) with recombinant SpCas9 and analysed the reactivity of  
81 CD3<sup>+</sup>4<sup>+</sup>8<sup>+</sup> T cells by flow cytometry with a set of markers for T cell activation (CD137, CD154) and  
82 effector cytokine production (IFN- $\gamma$ , TNF- $\alpha$ , IL-2) (Fig. 1a, b, Extended Data Fig 1).<sup>14,15</sup> We relied  
83 on protein uptake, processing and presentation of SpCas9 peptides by professional antigen-  
84 presenting cells (APCs) to both MHC I- and II within the PBMCs. Intriguingly, all donors evaluated  
85 showed specific memory/effector T cell activation upon SpCas9 stimulation indicated by CD137  
86 (4-1BB) upregulation in both, CD4 and CD8, T cell compartments (Fig. 1a, b, d, e, Extended Data  
87 Fig. 1). After subtraction of background an average of 0.28% (range 0.03-1.02 %) and 0.44 %  
88 (range 0.6-1.3%) expressed CD137 within CD4<sup>+</sup> and CD8<sup>+</sup> T cells, respectively (Fig. 1e). By  
89 multiparameter analysis at single cell level, we detected Cas9-specific multi-potent T<sub>EFF</sub>  
90 expressing at least one or even more effector cytokines (CD4<sup>+</sup> > CD8<sup>+</sup> T cells) (Fig 1b, c, f). The  
91 expression of the lymph node homing receptor CCR7 and the leucocyte common antigen isoform  
92 CD45RO allows for dissection of the reactive T cell subsets (Extended Data Fig. 2a).<sup>16</sup>  
93 Accordingly, we discovered that the majority of SpCas9-reactive T cells belongs to the effector-  
94 memory (CD4<sup>+</sup> and CD8<sup>+</sup>) and terminally differentiated effector memory effector cells (T<sub>EMRA</sub>)  
95 (CD8<sup>+</sup>) pool implying repetitive previous exposure to SpCas9, comparable with memory T cell  
96 response to the frequently reactivated cytomegalovirus (CMV) (Extended Data Fig. 2b-e).<sup>17</sup> The  
97 few cells within the naïve compartment might be related to stem cell memory T cell subset within  
98 this population.<sup>18</sup>

99 Our results imply a ubiquitous pre-primed T<sub>EFF</sub> response towards SpCas9, which could have  
100 immediate detrimental effects on tissues edited with a SpCas9-related system as those cells can

101 immediately migrate to the targeted tissue. However, CMV is reactivated repeatedly in lymphoid  
102 organs and tissues, while *S. pyogenes* show repeated/continuous colonization on body surfaces.  
103 Recent studies indicate, that continuous colonialization and repetitive exposure to environmental  
104 proteins or pathogens particularly at mucosal surfaces also induce T<sub>REG</sub>.<sup>19,20</sup> These T<sub>REG</sub> are  
105 required to balance immune responses or even to maintain tolerance against innocuous  
106 environmental antigens.<sup>20</sup> These findings expanded the significance of T<sub>REG</sub> from controlling auto-  
107 reactivity towards a general role for protection against tissue-damaging inflammation. To  
108 determine the relative contribution of T<sub>REG</sub> to the SpCas9-induced T cell response, we performed  
109 intracellular staining for the T<sub>REG</sub> lineage determining transcription factor FoxP3 in concert with  
110 CD25 surface expression.<sup>21,22</sup> Further, we combined those T<sub>REG</sub> defining markers with activation  
111 marker and cytokine profiling following SpCas9 whole protein stimulation (Fig. 2a, d, Extended  
112 Data Fig. 3). Intriguingly, we found excessive frequencies of T<sub>REG</sub> within SpCas9-reactive  
113 CD4<sup>+</sup>CD137<sup>+</sup> T cells ranging from 26.7-73.5% of total response (Fig. 2a, b). We confirmed T<sub>REG</sub>  
114 identity through additional phenotypic marker combinations like FoxP<sup>+</sup>CTLA-4<sup>+</sup> or  
115 CD127<sup>low</sup>CD25<sup>high</sup> (Fig. 2a, Extended Data Fig. 3a, b) and epigenetic analysis of the T<sub>REG</sub>-specific  
116 demethylation region (TSDR demethylation: T<sub>REG</sub> 83.7%; T<sub>EFF</sub> 1.87%; n=1).<sup>23,24</sup> Further  
117 investigation of the SpCas9-induced T cell activation revealed distinct T cell lineage determining  
118 transcription factor profiles. CD4<sup>+</sup>FoxP3<sup>+</sup> T<sub>REG</sub> were exclusively found within the CD137<sup>dim</sup>CD154<sup>-</sup>  
119 population, while CD4<sup>+</sup>Tbet<sup>+</sup> T<sub>EFF</sub> comprised both CD137<sup>+</sup>CD154<sup>+</sup> and CD137<sup>high</sup> SpCas9-  
120 responsive populations (Fig. 2c, Extended Data Fig. 4). Functionally, T<sub>REG</sub> did not contribute to  
121 SpCas9-induced effector cytokine production (Fig. 2d-f, Extended Data Fig. 5) but displayed a  
122 memory phenotype (Extended Data Fig. 3d). Taken together, our findings demonstrate that  
123 SpCas9-specific T<sub>REG</sub> are an inherent part of the physiological human SpCas9-specific T cell  
124 response.

125 Next, we investigated the individual relationship of T<sub>EFF</sub> and their T<sub>REG</sub> counterpart within the  
126 SpCas9-T cell response in comparison to an antiviral CMV and bacterial superantigen by relating  
127 the frequency of SpCas9, CMV phosphoprotein 65 (CMV<sub>pp65</sub>) and *Staphylococcus* Enterotoxin B  
128 (SEB)-activated T<sub>REG</sub> to those of T<sub>EFF</sub> within CD4<sup>+</sup>CD137<sup>+</sup> and T<sub>EFF</sub> within CD8<sup>+</sup>CD137<sup>+</sup> antigen-  
129 reactive T cells. Remarkably, we found a balanced effector/regulatory T cell response to SpCas9  
130 for both, CD4<sup>+</sup> and CD8<sup>+</sup>, T cell compartments while response to CMV<sub>pp65</sub> as well as SEB was  
131 dominated by T<sub>EFF</sub> (Fig. 3a, b). Intriguingly, frequency of SpCas9-reactive CD4<sup>+</sup>CD137<sup>+</sup>CD154<sup>-</sup>  
132 T<sub>REG</sub> cells inversely correlates with the magnitude of CD4<sup>+</sup>CD137<sup>+</sup>CD154<sup>+</sup> T<sub>EFF</sub> within the SpCas9-  
133 reactive CD4<sup>+</sup>CD137<sup>+</sup> T cells (Fig. 3c). In other words, our data show that donors with low SpCas9-  
134 reactive T<sub>REG</sub> have relatively higher T<sub>EFF</sub> response to SpCas9 suggesting that the level of SpCas9-  
135 specific T<sub>EFF</sub> response might be controlled by SpCas9-specific T<sub>REG</sub>. A misbalanced SpCas9-

136 reactive  $T_{REG}/T_{EFF}$  ratio may result in an overwhelming effector immune response to SpCas9  
137 following *in vivo* CRISPR/Cas9 gene editing.

138 Several preclinical and first clinical data show that adoptively transferred  $T_{REG}$  are able to combat  
139 not only T cell priming but also overwhelming  $T_{EFF}$  response.<sup>25,26</sup> Therefore, SpCas9-specific  $T_{REG}$   
140 may have the potential to mitigate a SpCas9-directed  $T_{EFF}$  response. Having demonstrated that  
141 some individuals have a relatively low SpCas9-specific  $T_{REG}/T_{EFF}$  ratio, adoptive transfer of those  
142 cells would be an option. Therefore, we tested enrichment and *in vitro* expansion of both SpCas9-  
143 specific  $T_{EFF}$  and  $T_{REG}$  (Extended Data Fig. 6). To examine their SpCas9-specific effector function,  
144 we re-stimulated  $T_{EFF}$  lines with SpCas9-loaded APCs after expansion and detected pronounced  
145 effector cytokine production (Extended Data Fig. 7). Notably, most cells within the SpCas9-specific  
146  $T_{REG}$  lines lost their  $T_{REG}$ -specific phenotype when cultured with IL-2, but were stabilized in the  
147 presence of the mTOR-inhibitor rapamycin, which is commonly used for expansion of thymic-  
148 derived naturally occurring  $T_{REG}$ .<sup>27</sup>

149 What might be the physiological significance of a relatively high frequency of SpCas9-specific  $T_{REG}$   
150 compared to CMV/SEB? Bacterial colonization requires homeostasis between the host and the  
151 microbiota for optimal coexistence. This interplay is tightly mediated by microbe-specific  $T_{REG}$ .  
152 Prominently, patients suffering from immunodysregulation polyendocrinopathy enteropathy X-  
153 linked (IPEX) syndrome lacking functional  $T_{REG}$  cells fail to establish a healthy commensal flora  
154 resulting in multiple immunopathologies.<sup>28</sup> Interestingly, *S. pyogenes* infection-associated  
155 diseases leading to systemic complications like rheumatic fever, occur predominantly in children  
156 and during adolescence.<sup>12</sup> The pathophysiology is believed to involve molecular mimicry inducing  
157 cross-reactive antibodies by T helper cells ( $T_H$ ).<sup>29</sup> However,  $T_H$  mediated inflammation is controlled  
158 by  $T_{REG}$ . Therefore, it would be worth to prove whether a misbalanced *S. pyogenes*-specific  
159  $T_{REG}/T_{EFF}$  response may be related to *S. pyogenes*-associated diseases.

160 In conclusion, our findings imply the requirement for controlling SpCas9  $T_{EFF}$  response for  
161 successful CRISPR/Cas9 gene editing *in vivo*. It remains to be elucidated whether SpCas9-  
162 directed T cells can migrate into tissues relevant for gene therapy. Our results emphasize the  
163 necessity of stringent immune monitoring of SpCas9-specific T cell responses, preceding and  
164 accompanying clinical trials employing Cas9-derived therapeutic approaches to identify potentially  
165 high-risk patients. Henceforth, misbalanced  $T_{REG}/T_{EFF}$  ratios and strong  $CD8^+$  T cell responses to  
166 SpCas9 may exclude patients for Cas9-associated gene-therapy. Gene editing with only transient  
167 SpCas9 exposure may reduce the risk for hazardous immunogenicity events. In contrast,  
168 technologies relying on *ex vivo* modification will not have a problem with immunogenicity because  
169 the gene-edited cells can be infused after complete degradation of the Cas9 protein.  
170 Unresponsiveness of autologous SpCas9-specific  $T_{EFF}$  lines to stimulation with CRISPR/Cas9-

171 edited cell samples could be a release criterion for cell/tissue products in CRISPR/Cas9-related  
172 gene therapy (Extended Data Fig. 7). For *in vivo* application of CRISPR/Cas9,  
173 immunosuppressive treatment must be considered, especially if the control by T<sub>REG</sub> is insufficient  
174 due to low T<sub>REG</sub>/T<sub>EFF</sub> ratio. Immunosuppressive drugs discussed for AAV-related gene therapy in  
175 naïve recipients, such as CTLA4-IgG and low dose prednisone, are inadequate to control a pre-  
176 existing T<sub>EFF</sub> response.<sup>30</sup> Adoptive transfer of SpCas9-specific T<sub>REG</sub> should be considered as an  
177 approach to prevent hazardous inflammatory damage to CRISPR/Cas9-edited tissues and would  
178 circumvent the need for global immunosuppression.

179

180

181 **Materials and Methods**

182

183 **Cell preparation**

184 We collected blood samples from healthy volunteers after obtaining informed consent. We  
185 separated PBMCs from heparinized whole blood from healthy donors at different days (median  
186 age: 30, range: 18-57, 12 female/ 12 male) by lymphoprep density gradient centrifugation with a  
187 Biocoll-separating solution. PBMCs were cultured in complete medium, comprising VLE-RPMI  
188 1640 medium supplemented with stable glutamine, 100 U/ml penicillin, 0.1 mg/ml streptomycin  
189 (all from Biochrom, Berlin, Germany) and 10% heat-inactivated FCS (PAA).

190

191 **Flow cytometry analysis**

192 We stimulated freshly isolated PBMCs in polystyrene round bottom tubes (Falcon, Corning) at 37  
193 °C in humidified incubators and 5% CO<sub>2</sub> for 16 h with the following antigens: 8 µg/ml Streptococcus  
194 pyogenes (Sp) CRISPR associated protein 9 (Cas9) (SpCas9) (PNA Bio Inc., CA, USA), 1 µg/ml  
195 SEB (Sigma) and CMV<sub>pp65</sub> overlapping peptide pool at 1 µg/ml (15mer, 11 aa overlap, JPT Peptide  
196 Technologies, Berlin, Germany). For functional and phenotypic characterisation, 5x10<sup>6</sup> PBMC / 1  
197 ml complete medium were stimulated. For analysis of antigen-induced intracellular CD154 and  
198 CD137 expression and IFN- $\gamma$ , TNF- $\alpha$  and IL-2 production, we added 2 µg/ml Brefeldin A (Sigma).  
199 To allow for sufficient SpCas9 antigenic APC processing and presentation, Brefeldin A was added  
200 for the last 10 h of stimulation. After harvesting, extracellular T cell memory phenotype staining  
201 was performed using fluorescently conjugated monoclonal antibodies for CCR7 (PE, clone:  
202 G043H7), CD45RA (PE-Dazzle 594, clone: HI100) and CD45RO (BV785, clone: UCHL1) for 30  
203 min at 4 °C. In certain experiments CD25 (BD, APC, clone: 2A3), CD127 (Beckman Coulter, APC-  
204 Alexa Fluor 700, clone: R34.34) and CD152 (CTLA-4) (BD, PE-Cy5, clone: BNI3) antibodies were  
205 used to define T<sub>REG</sub> specific surface molecule expression. To exclude dead cells, LIVE/DEAD  
206 Fixable Blue Dead Stain dye (Invitrogen) was added. Subsequently, cells were fixed and  
207 permeabilised with FoxP3/Transcription factor staining buffer set (eBioscience) according to the  
208 manufacturer's instructions. After washing, we stained fixed cells for 30 min at 4 °C with the  
209 following monoclonal antibodies: FoxP3 (Alexa Fluor 488, clone: 259D), CD3 (BV650, clone:  
210 OKT3), CD4 (PerCp-Cy5.5, clone: SK3) CD8 (BV570, clone: RPA-T8), CD137 (PE-Cy7, clone:  
211 4B4-4), CD154 (BV711, clone 24-31), IFN- $\gamma$  (BV605, clone 4S.B3), TNF- $\alpha$  (Alexa Fluor 700, clone:  
212 MAb11) and IL-2 (BV421, clone MQ1-17H12)). In particular experiments, antibodies for  
213 intracellular fluorescence staining of Tbet (Alexa Fluor 647, clone: 4B10) and FoxP3 were used to  
214 define T cell lineage determining transcription factor expression levels. All antibodies were  
215 purchased from Biolegend, unless indicated otherwise. Cells were analysed on a LSR-II Fortessa

216 flow cytometer (BD Biosciences) and FlowJo Version 10 software (Tree Star). For *ex vivo* analysis,  
217 at least  $1 \times 10^6$  events were recorded. Lymphocytes were gated based on the FSC versus SSC  
218 profile and subsequently gated on FSC (height) versus FSC to exclude doublets. Unstimulated  
219 PBMC were used as controls and respective background responses have been subtracted from  
220 SpCas9 or CMV<sub>pp65</sub>-specific cytokine production (Fig. 1d). Negative values were set to zero.

221

## 222 **SpCas9-specific T cell isolation and expansion**

223 *Isolation:* We separated PBMCs from 80 mL heparinized whole blood. We washed PBMCs twice  
224 with PBS and cultured them for 16 h at 37 °C in humidified incubators and 5% CO<sub>2</sub> in the presence  
225 of 8 µg/ml SpCas9 whole protein and 1 µg/ml CD40-specific antibody (Miltenyi Biotech, HB 14) at  
226 cell concentrations of  $1 \times 10^7$  PBMCs per 2 mL VLE-RPMI 1640 medium with stable glutamine  
227 supplemented with 100 U/ml penicillin, 0.1 mg/ml streptomycin and 5% heat-inactivated human  
228 AB serum (PAA) in polystyrene flat bottom 24 well plates (Falcon, Corning). After stimulation, cells  
229 were washed with PBS (0.5% BSA) and stained for 10 minutes with BV650-conjugated CD3-  
230 specific antibody, PerCp-Cy5.5-conjugated CD4-specific antibody, APC-conjugated CD25-  
231 specific antibody, APC-Alexa Fluor 700-conjugated CD127-specific antibody (Beckman Coulter),  
232 PE-Cy7-conjugated CD137-specific antibody and BV711-conjugated CD154-specific antibody.  
233 SpCas9-specific T<sub>REG</sub> (Extended Data Fig. 6a: CD3<sup>+</sup>CD4<sup>+</sup>CD137<sup>+</sup>CD154<sup>-</sup>CD25<sup>high</sup>CD127<sup>-</sup>) and  
234 SpCas9-specific T<sub>EFF</sub> (Extended Data Fig. 6a: CD3<sup>+</sup>CD137<sup>+</sup>CD154<sup>+</sup>CD25<sup>low</sup>) were enriched by  
235 fluorescently activated cell sorting on a BD FACSAriaII SORP (BD Biosciences). In addition,  
236 polyclonal (pc) T<sub>REG</sub> (Extended Data Fig. 6a: CD3<sup>+</sup>CD4<sup>+</sup>CD137<sup>-</sup>CD154<sup>-</sup>CD25<sup>high</sup>CD127<sup>-</sup>) and pc  
237 T<sub>EFF</sub> (Extended Data Fig. 6a: CD3<sup>+</sup>CD137<sup>+</sup>CD154<sup>+</sup>CD25<sup>low</sup>) were enriched for non-specific  
238 expansion. Intracellular T<sub>REG</sub>-specific FoxP3 transcription factor staining was performed post-  
239 sorting. Post-sorting analysis of purified subsets revealed greater than 90% purity.

240 *Expansion:* We cultured isolated SpCas9-specific T<sub>EFF</sub> and control pc T<sub>EFF</sub> cells at 37 °C in  
241 humidified incubators and 5% CO<sub>2</sub> at a ratio of 1:50 with irradiated autologous PBMC (30 Gy) in a  
242 96-well plate (Falcon, Corning) with RPMI medium containing 5% human AB serum including 50  
243 U/mL recombinant human (rh) IL-2 (Proleukin, Novartis). Isolated SpCas9-specific T<sub>REG</sub> cells were  
244 cultured at 37 °C in humidified incubators and 5% CO<sub>2</sub> at a ratio of 1:50 with irradiated autologous  
245 PBMC (30 Gy) in a 96-well plate with X-Vivo 15 Medium (Lonza) containing 5% human AB serum  
246 including 500 U/mL rh IL-2 in the presence or absence of 100nM rapamycin (Pfizer). Non-specific  
247 pc T<sub>REG</sub> were activated for polyclonal expansion applying the T<sub>REG</sub> expansion kit according to the  
248 manufacturer's instructions (T<sub>REG</sub> : bead ratio of 1:1; CD3/CD28 MACSiBead particles, Miltenyi  
249 Biotech, Germany) and cultured in X-Vivo 15 Medium in the presence of 100nM rapamycin. We  
250 isolated a minimum of  $10^4$  SpCas9-specific CD137<sup>+</sup>CD154<sup>-</sup> T<sub>REG</sub> cells, which could be expanded

251 in vitro to at least  $10^5$  cells within 10 days. Medium and cytokines were added every other day or  
252 when cells were split during expansion.

253

#### 254 ***In vitro* restimulation of ex vivo isolated and expanded SpCas9-specific T cells**

255 Cultured SpCas9-specific T<sub>EFF</sub> and T<sub>REG</sub> were analysed at day 10 for expression of effector  
256 molecules in response to stimulation with SpCas9 whole protein-loaded autologous monocyte-  
257 derived dendritic cells (moDCs). CD14<sup>+</sup> monocytes were enriched from PBMCs by magnetically  
258 activated cell sorting (MACS, Miltenyi Biotech). Subsequently, CD14<sup>+</sup> cells were cultured for 5  
259 days in 1,000IU/mL rhGM-CSF (Cellgenix) and 400IU/mL rhIL-4 (Cellgenix). Then, fresh medium  
260 with 1,000IU/ml TNF- $\alpha$  (Cellgenix) was supplied. During 48 h of TNF- $\alpha$  induced maturation of  
261 autologous moDCs 4  $\mu$ g/ml SpCas9 was added. We re-stimulated expanded T cell subsets with  
262 either SpCas9-pulsed, 1  $\mu$ g/ml CMV<sub>pp65</sub> overlapping peptide pool-pulsed or un-pulsed autologous  
263 moDCs for 6 h at a ratio of 10:1. 2  $\mu$ g/ml Brefeldin A was added for the last 5 h of stimulation.  
264 Following stimulation, we analysed the expression of CD3, CD4, CD8, CD25, intracellular IFN- $\gamma$ ,  
265 TNF- $\alpha$  and IL-2, and intra-nuclear FoxP3, and treated the cells for flow cytometric readout as  
266 described above. We stained cells with BV650-conjugated CD3-specific antibody, PerCp-Cy5.5-  
267 conjugated CD4-specific antibody, BV570-conjugated CD8-specific antibody, APC-conjugated  
268 CD25-specific antibody, BV605 conjugated IFN- $\gamma$ -specific antibody, Alexa Fluor 700 conjugated  
269 TNF- $\alpha$ -specific antibody and BV421-conjugated IL-2-specific antibody.

270

#### 271 **TSDR – Methylation analysis**

272 DNA methylation analysis of the T<sub>REG</sub>-specific demethylation region (TSDR) was performed as  
273 previously described.<sup>24</sup> Briefly, bisulfite-modified genomic DNA (Quick-DNA Miniprep Plus Kit,  
274 Zymo Research, Irvine, USA; EpiTect Bisulfite Kit, Qiagen, Hilden, Germany) was used in a real-  
275 time polymerase chain reaction for FoxP3 TSDR quantification. A minimum of 40 ng genomic DNA  
276 or a respective amount of plasmid standard was used in addition to 10  $\mu$ l FastStart Universal  
277 Probe Master (Roche Diagnostics, Mannheim, Germany), 50 ng/ $\mu$ l Lambda DNA (New England  
278 Biolabs, Frankfurt, Germany), 5 pmol/ $\mu$ l methylation or nonmethylation-specific probe, 30 pmol/ $\mu$ l  
279 methylation or nonmethylation-specific primers (both from Epiontis, Berlin, Germany) in 20  $\mu$ l total  
280 reaction volume. The samples were analysed in triplicate on an ABI 7500 cycler (Life Technologies  
281 Ltd, Carlsbad, USA).

282

283

284

285 **Statistical analysis and calculations**

286 Graph Pad Prism version 7 was used for generation of graphs and statistical analysis. To test for  
287 normal Gaussian distribution Kolmogorov-Smirnov test, D'Agostino & Pearson normality test and  
288 Shapiro-Wilk normality test were performed. In two data set comparisons, if data were normally  
289 distributed Student's paired t test was employed for analysis. If data were not normally distributed  
290 Wilcoxon's matched pairs test was applied. All tests were two-tailed. Where we compared more  
291 than two paired data sets, one way ANOVA was employed for normally distributed samples and  
292 Friedman's test was used for not normally distributed samples. For comparison of more than two  
293 unpaired not normally distributed data sets, we applied Kruskal-Wallis' test. To exactly identify  
294 significant differences in not normally distributed data sets Dunn's multiple comparison test was  
295 used as post-test and the post-test employed for normally distributed samples was Tukey's  
296 multiple comparison test. Correlation analysis was assessed by Pearson's correlation coefficients  
297 for normally distributed data or non-parametric Spearman's rank correlation for not normally  
298 distributed data. The regression line was inserted based on linear regression analysis. Probability  
299 (p) values of  $\leq 0.05$  were considered statistically significant and significance is denoted as follows:  
300 \* =  $p \leq 0.05$ ; \*\* =  $p \leq 0.01$ ; \*\*\* =  $p \leq 0.001$ ; \*\*\*\* =  $p \leq 0.0001$ .

301

302

303 **Acknowledgments**

304 We would like to acknowledge the assistance of the BCRT Flow Cytometry Core Lab, Dr. D.  
305 Kunkel and J. Hartwig.

306

307

308 **Disclosures**

309 The authors have no financial conflicts of interest.

310

311

312 **Author contributions**

313 D.L.W. led the project, designed the research, performed most of the experiments, analysed and  
314 interpreted the data, and wrote the manuscript. L.A. and D.J.W. established methods, performed  
315 some of the experiments and revised the manuscript. P.R. wrote the manuscript and supplied  
316 reagents. H.-D.V. designed the research, interpreted the data and wrote the manuscript. M.S.-H.  
317 led the project, designed the research, analysed and interpreted the data, and wrote the  
318 manuscript.

319

320 **Bibliography**

- 321 1. Jinek, M. *et al.* A Programmable Dual-RNA-Guided DNA Endonuclease in Adaptive  
322 Bacterial Immunity. *Science* (80-. ). **337**, 816–821 (2012).
- 323 2. Cox, D. B. T., Platt, R. J. & Zhang, F. Therapeutic genome editing: prospects and  
324 challenges. *Nat. Med.* **21**, 121–131 (2015).
- 325 3. Lehrman, S. Virus treatment questioned after gene therapy death. *Nature* **401**, 517  
326 (1999).
- 327 4. Nayak, S. & Herzog, R. W. Progress and prospects: immune responses to viral vectors.  
328 *Gene Ther.* **17**, 295–304 (2010).
- 329 5. Chew, W. L. Immunity to CRISPR Cas9 and Cas12a therapeutics. *Wiley Interdiscip. Rev.*  
330 *Syst. Biol. Med.* **10**, e1408 (2017).
- 331 6. Chew, W. L. *et al.* A multifunctional AAV–CRISPR–Cas9 and its host response. *Nat.*  
332 *Methods* **13**, 868–874 (2016).
- 333 7. Fu, Y. *et al.* High-frequency off-target mutagenesis induced by CRISPR-Cas nucleases in  
334 human cells. *Nat. Biotechnol.* **31**, 822–6 (2013).
- 335 8. Chen, J. S. *et al.* Enhanced proofreading governs CRISPR–Cas9 targeting accuracy.  
336 *Nature* (2017). doi:10.1038/nature24268
- 337 9. Komor, A. C., Kim, Y. B., Packer, M. S., Zuris, J. A. & Liu, D. R. Programmable editing of  
338 a target base in genomic DNA without double-stranded DNA cleavage. *Nature* **533**, 420–  
339 424 (2016).
- 340 10. Thakore, P. I., Black, J. B., Hilton, I. B. & Gersbach, C. A. Editing the epigenome:  
341 technologies for programmable transcription and epigenetic modulation. *Nat. Methods* **13**,  
342 127–37 (2016).
- 343 11. Shaikh, N., Leonard, E. & Martin, J. M. Prevalence of Streptococcal Pharyngitis and  
344 Streptococcal Carriage in Children: A Meta-analysis. *Pediatrics* **126**, e557–e564 (2010).
- 345 12. Carapetis, J. R., Steer, A. C., Mulholland, E. K. & Weber, M. The global burden of group A  
346 streptococcal diseases. *Lancet Infect. Dis.* **5**, 685–694 (2005).
- 347 13. Charlesworth, C. T. *et al.* Identification of Pre-Existing Adaptive Immunity to Cas9  
348 Proteins in Humans. *bioRxiv* 243345 (2018). doi:10.1101/243345
- 349 14. Frensch, M. *et al.* Direct access to CD4+ T cells specific for defined antigens according to  
350 CD154 expression. *Nat. Med.* **11**, 1118–1124 (2005).
- 351 15. Wolf, M. *et al.* Activation-induced expression of CD137 permits detection, isolation, and  
352 expansion of the full repertoire of CD8+ T cells responding to antigen without requiring  
353 knowledge of epitope specificities. *Blood* **110**, 201–10 (2007).
- 354 16. Sallusto, F., Lenig, D., Förster, R., Lipp, M. & Lanzavecchia, A. Two subsets of memory T

- 355 lymphocytes with distinct homing potentials and effector functions. *Nature* **401**, 708–712  
356 (1999).
- 357 17. Schmueck-Henneresse, M. *et al.* Peripheral Blood-Derived Virus-Specific Memory Stem T  
358 Cells Mature to Functional Effector Memory Subsets with Self-Renewal Potency. *J.*  
359 *Immunol.* (2015). doi:10.4049/jimmunol.1402090
- 360 18. Gattinoni, L. *et al.* A human memory T cell subset with stem cell-like properties. *Nat. Med.*  
361 **17**, 1290–7 (2011).
- 362 19. Lathrop, S. K. *et al.* Peripheral education of the immune system by colonic commensal  
363 microbiota. *Nature* **478**, 250–254 (2011).
- 364 20. Bacher, P. *et al.* Regulatory T Cell Specificity Directs Tolerance versus Allergy against  
365 Aeroantigens in Humans. *Cell* **167**, 1067–1078.e16 (2016).
- 366 21. Sakaguchi, S., Sakaguchi, N., Asano, M., Itoh, M. & Toda, M. Immunologic self-tolerance  
367 maintained by activated T cells expressing IL-2 receptor alpha-chains (CD25). Breakdown  
368 of a single mechanism of self-tolerance causes various autoimmune diseases. *J.*  
369 *Immunol.* **155**, 1151–64 (1995).
- 370 22. Hori, S., Nomura, T. & Sakaguchi, S. Control of Regulatory T Cell Development by the  
371 Transcription Factor Foxp3. *Science* (80-. ). **299**, 1057–1061 (2003).
- 372 23. Wing, K. *et al.* CTLA-4 Control over Foxp3+ Regulatory T Cell Function. *Science* (80-. ).  
373 **322**, 271–275 (2008).
- 374 24. Wieczorek, G. *et al.* Quantitative DNA Methylation Analysis of FOXP3 as a New Method  
375 for Counting Regulatory T Cells in Peripheral Blood and Solid Tissue. *Cancer Res.* **69**,  
376 599–608 (2009).
- 377 25. Lei, H., Schmidt-Bleek, K., Dienelt, A., Reinke, P. & Volk, H.-D. Regulatory T cell-  
378 mediated anti-inflammatory effects promote successful tissue repair in both indirect and  
379 direct manners. *Front. Pharmacol.* **6**, 184 (2015).
- 380 26. Chandran, S. *et al.* Polyclonal Regulatory T Cell Therapy for Control of Inflammation in  
381 Kidney Transplants. *Am. J. Transplant.* **17**, 2945–2954 (2017).
- 382 27. Battaglia, M., Stabilini, A. & Roncarolo, M.-G. Rapamycin selectively expands  
383 CD4+CD25+FoxP3+ regulatory T cells. *Blood* **105**, 4743–4748 (2005).
- 384 28. Ochs, H. D. *et al.* The immune dysregulation, polyendocrinopathy, enteropathy, X-linked  
385 syndrome (IPEX) is caused by mutations of *FOXP3*. *Nat. Genet.* **27**, 20–21 (2001).
- 386 29. Guilherme, L., Kalil, J. & Cunningham, M. Molecular mimicry in the autoimmune  
387 pathogenesis of rheumatic heart disease. *Autoimmunity* **39**, 31–39 (2006).
- 388 30. Arruda, V. R., Favaro, P. & Finn, J. D. Strategies to modulate immune responses: a new  
389 frontier for gene therapy. *Mol. Ther.* **17**, 1492–503 (2009).

390

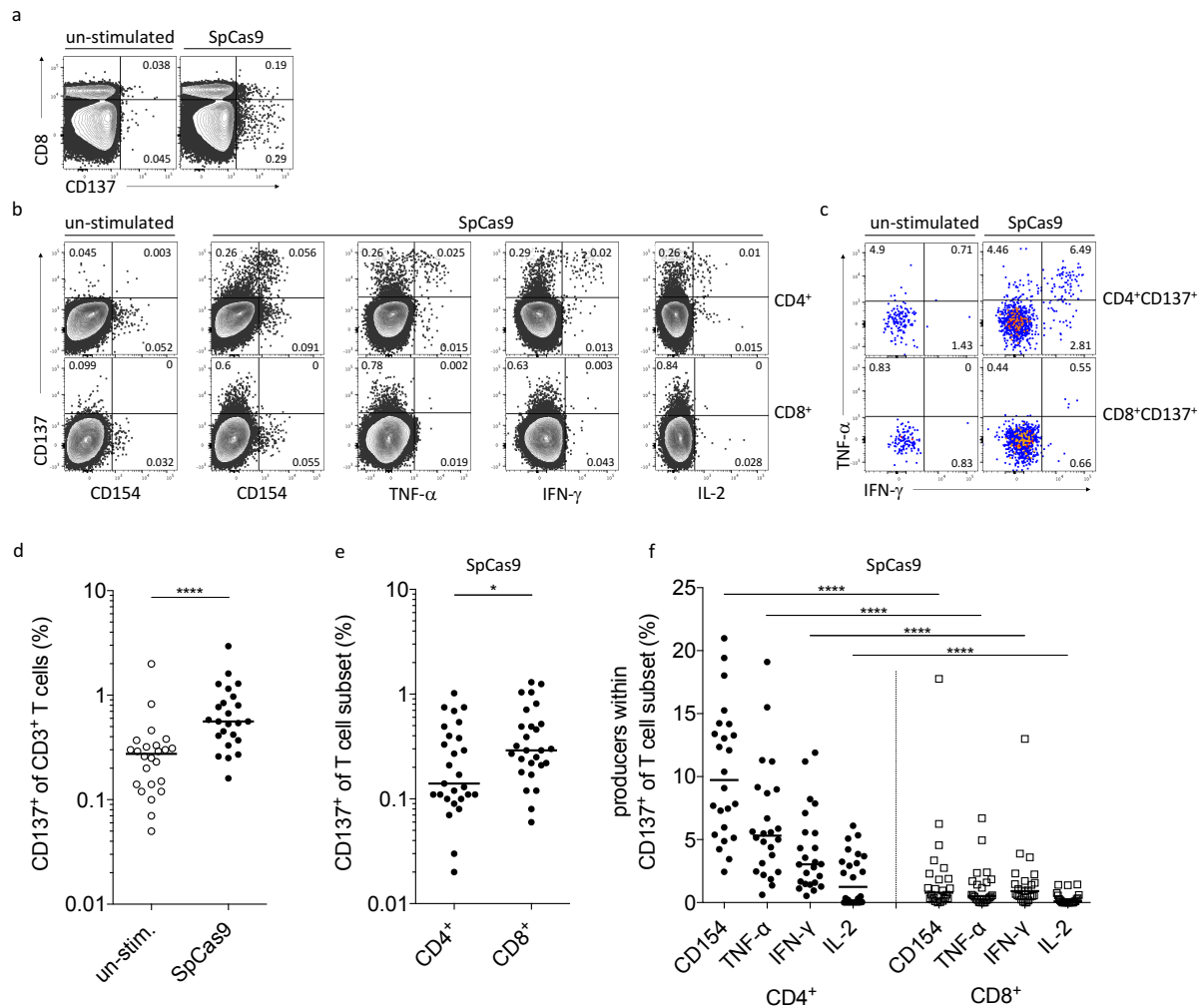


**Figure 1. Ubiquitous peripheral SpCas9-specific T cell response within human donors.**

SpCas9-specific human CD3<sup>+</sup> T cells can be identified after short-term *ex vivo* stimulation. PBMCs were stimulated with SpCas9 whole protein for 16 h. Frequencies of T cell response were assessed by flow cytometry. (a) Representative FACS plots show SpCas9-induced activation defined by CD137 expression of CD8<sup>+</sup> and CD8<sup>-</sup> T cells in comparison to unstimulated control. (b) Gating of single alive CD3<sup>+</sup> T cells and dissection into CD4<sup>+</sup> and CD8<sup>+</sup> T cells. Representative FACS plots of SpCas9-induced CD137 and CD154 expression as well as IFN- $\gamma$ , TNF- $\alpha$  and IL-2 production are shown. (c) Representative FACS plots of IFN- $\gamma$  and TNF- $\alpha$  production within SpCas9-activated CD4<sup>+</sup>CD137<sup>+</sup> and CD8<sup>+</sup>CD137<sup>+</sup> T cells. (d) Paired analysis of SpCas9-induced CD137 expression within peripheral CD3<sup>+</sup> T cells compared to unstimulated controls. (e) Background subtracted CD137 expression to SpCas9 whole protein by CD4<sup>+</sup> and CD8<sup>+</sup> T cells. (f) SpCas9-induced expression of CD154, TNF- $\alpha$ , IFN- $\gamma$  and IL-2 within activated CD4<sup>+</sup>CD137<sup>+</sup> and CD8<sup>+</sup>CD137<sup>+</sup> T cells. (n=24; horizontal lines within graphs indicate medians.)

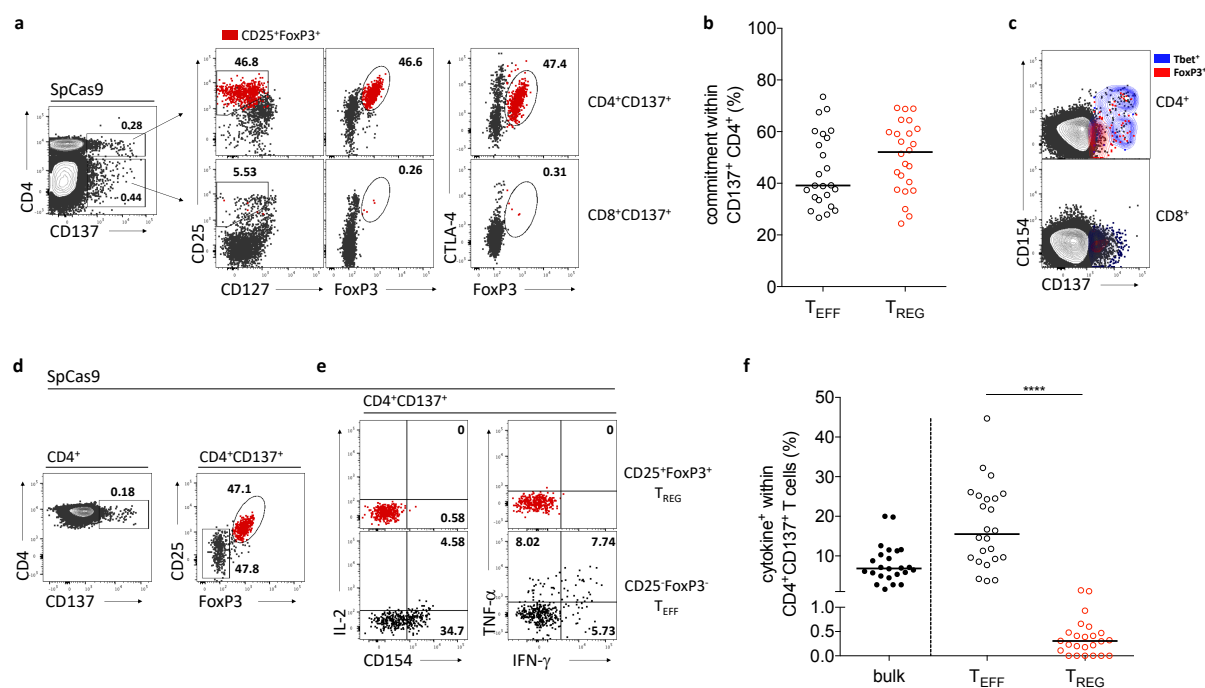


## Figure 2. SpCas9-specific T cell response contains a substantial proportion of regulatory T cells.

Identification of T<sub>EFF</sub> and T<sub>REG</sub> phenotypes within CD137<sup>+</sup> T cells after 16 h stimulation of human PBMCs with SpCas9 whole protein. **(a)** Representative FACS plots show FoxP3 expression of T<sub>REG</sub>-defining markers CD25, FoxP3, CTLA-4 and CD127 within SpCas9-activated CD4<sup>+</sup>CD137<sup>+</sup> and CD4<sup>-</sup>CD137<sup>+</sup> T cells. The overlay highlighted in red represents CD25<sup>+</sup>FoxP3<sup>+</sup> of CD137<sup>+</sup> T cells. **(b)** Contribution to SpCas9-induced CD4<sup>+</sup>CD137<sup>+</sup> T cell response by T<sub>EFF</sub> and CD25<sup>+</sup>FoxP3<sup>+</sup> T<sub>REG</sub> phenotypes. **(c)** Overlay contour plots of a representative donor demonstrate Tbet<sup>+</sup> (blue) and FoxP3<sup>+</sup> (red) T cells within SpCas9-induced T cell activation defined by CD137 and CD154 expression. **(d)** Gating of CD4<sup>+</sup>T<sub>REG</sub> within SpCas9-induced CD4<sup>+</sup>CD137<sup>+</sup> T cells and **(e)** corresponding CD154 expression and cytokine production within CD4<sup>+</sup>CD137<sup>+</sup> T<sub>REG</sub> (red) and T<sub>EFF</sub> (black). **(f)** Summary of accumulated cytokine production within bulk CD4<sup>+</sup>CD137<sup>+</sup> T cells, CD4<sup>+</sup>CD137<sup>+</sup> T<sub>EFF</sub> (CD25<sup>-</sup>FoxP3<sup>-</sup>) and CD4<sup>+</sup>CD137<sup>+</sup> T<sub>REG</sub> (CD25<sup>+</sup>FoxP3<sup>+</sup>). (n=24; horizontal lines within graphs indicate median values.)

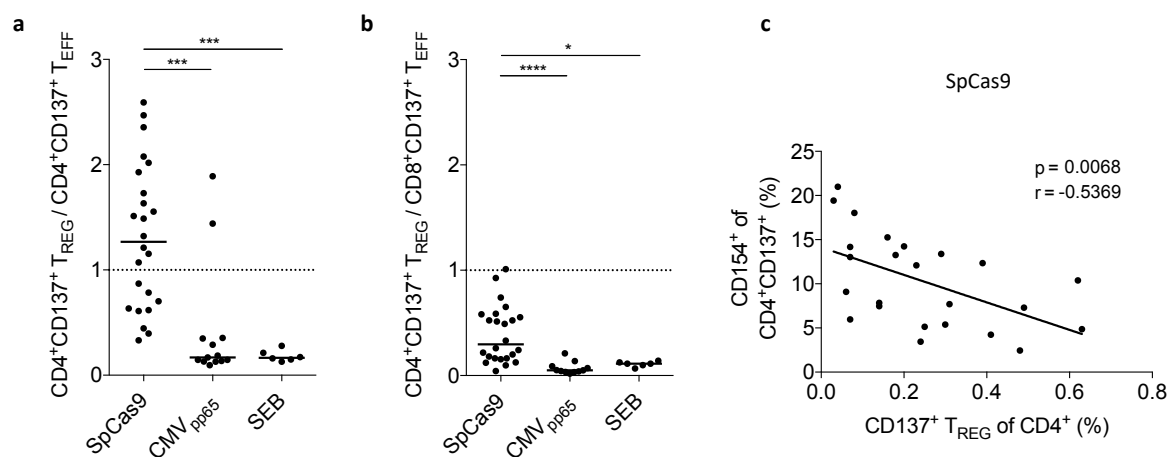
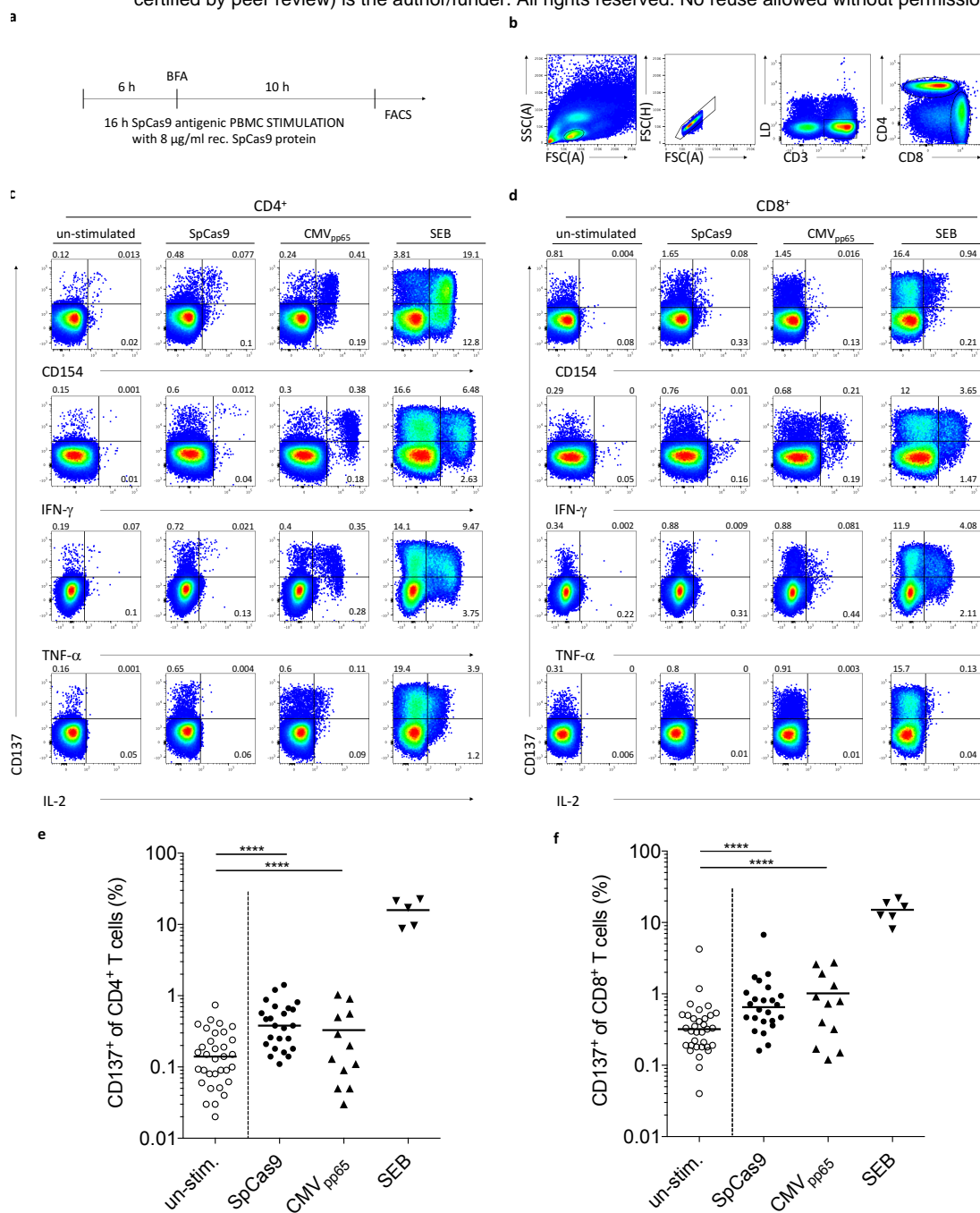


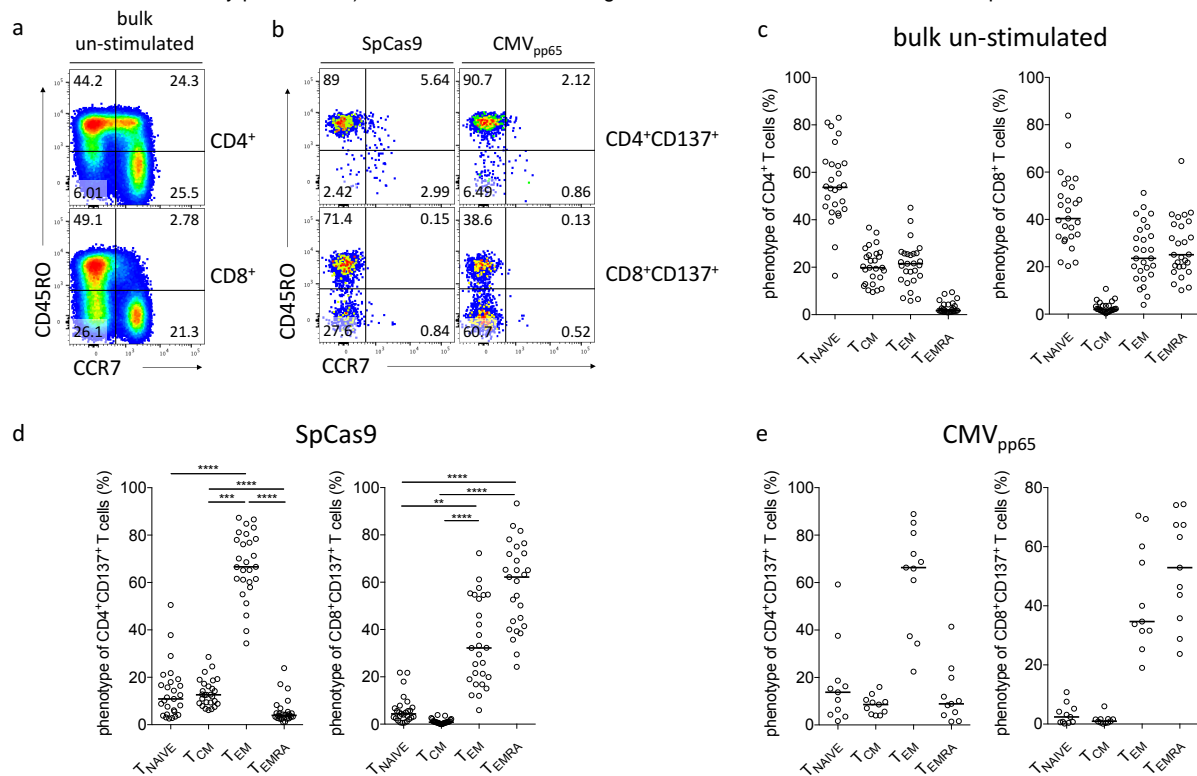
**Figure 3. A balanced effector/regulatory T cell response to SpCas9 whole protein.**

(a) Relation of antigen-reactive T<sub>REG</sub> to CD4<sup>+</sup>T<sub>EFF</sub> shown for SpCas9 whole protein, CMV<sub>pp65</sub> peptides and SEB stimulation. Antigen-reactive T<sub>REG</sub> and T<sub>EFF</sub> were defined according to gating strategy presented in Fig. 2d. Ratio was calculated by dividing the frequency of T<sub>REG</sub> by the proportion of T<sub>EFF</sub> within CD4<sup>+</sup>CD137<sup>+</sup> antigen-reactive cells. (b) Relation of antigen-reactive T<sub>REG</sub> to CD8<sup>+</sup>T<sub>EFF</sub> shown for SpCas9 whole protein, CMV<sub>pp65</sub> peptides and SEB stimulation. Ratio was calculated by dividing the frequency of T<sub>REG</sub> by the proportion of T<sub>EFF</sub> within CD4<sup>+</sup>CD137<sup>+</sup> antigen-reactive cells. (c) Inverse correlation of SpCas9-reactive T<sub>REG</sub> and SpCas9-reactive CD4<sup>+</sup>CD137<sup>+</sup>CD154<sup>+</sup> T<sub>EFF</sub>. Pearson correlation coefficients were computed between frequency of SpCas9-reactive CD4<sup>+</sup>CD137<sup>+</sup> T<sub>REG</sub> within total CD4<sup>+</sup> and the proportion of CD154<sup>+</sup> cells within the SpCas9-activated CD4<sup>+</sup>CD137<sup>+</sup> T cell pool. (SpCas9: n=24, CMV<sub>pp65</sub>: n=12, SEB: n=6. Horizontal lines within graphs indicate median values.)



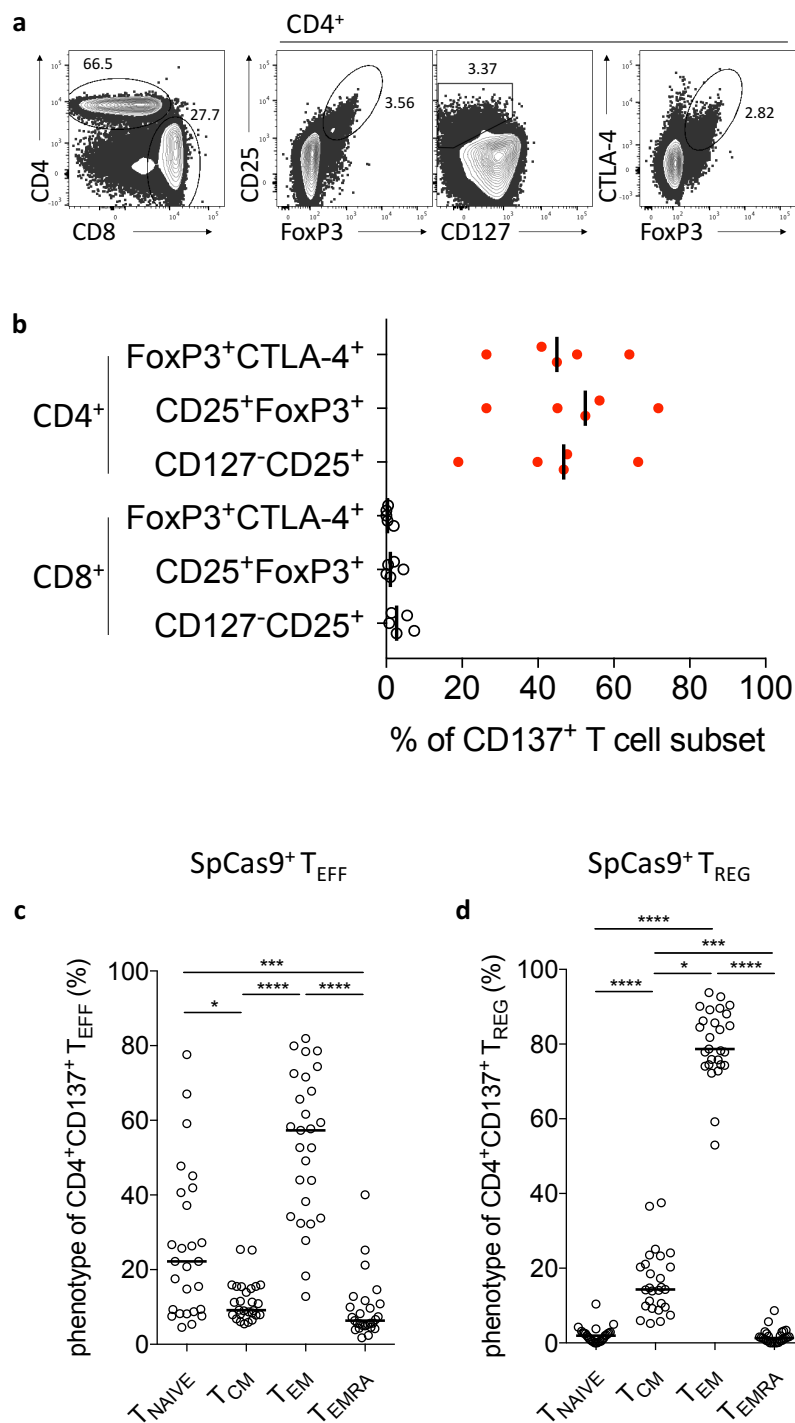
**Extended Data Figure 1. *Ex vivo* stimulation with SpCas9 whole protein induces polyfunctional effector CD4<sup>+</sup> and CD8<sup>+</sup> T cell responses.**

**(a)** Experimental design for *ex vivo* detection of SpCas9-specific T cell responses. **(b)** Representative gating strategy for defining alive CD3<sup>+</sup>CD4<sup>+</sup> and CD3<sup>+</sup>CD8<sup>+</sup> T lymphocytes. Lymphocytes were gated based on the FSC *versus* SSC profile and subsequently gated on FSC (height) *versus* FSC to exclude doublets. **(c and d;** summarized in **e and f**) Representative FACS images show SpCas9-induced activation defined by CD137 expression plotted against CD154, IFN- $\gamma$ , TNF- $\alpha$  and IL-2 for CD4<sup>+</sup> and CD8<sup>+</sup> T cells in comparison to CMV<sub>pp65</sub>-stimulated and SEB-stimulated PBMCs. (SpCas9: n=24, CMV<sub>pp65</sub>: n=12, SEB: n=6. Horizontal lines within graphs indicate medians.)



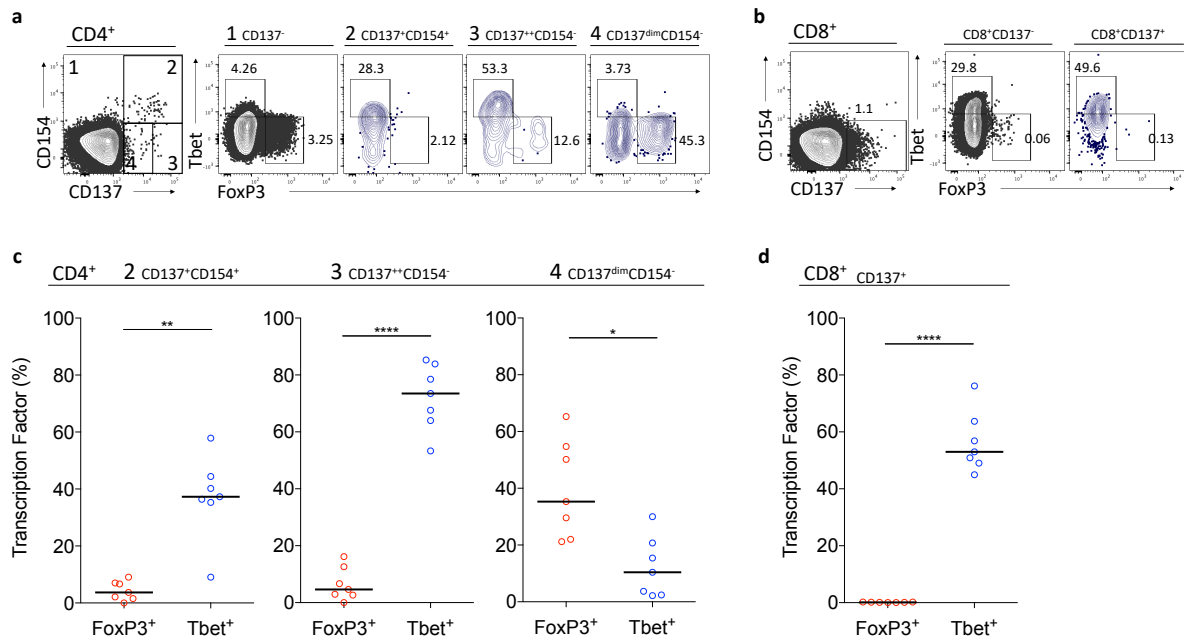
### Extended Data Figure 2. SpCas9- and viral CMV<sub>pp65</sub>-reactive CD4<sup>+</sup> and CD8<sup>+</sup> T cells phenotypically show a memory profile.

(a) Strategy for defining T cell subsets from PBMCs according to the expression of CD3<sup>+</sup> CD45RO<sup>+</sup> and CCR7<sup>+</sup> within CD4<sup>+</sup> and CD8<sup>+</sup> T cells. Dissection of the T cell differentiation profile into the following subsets: Naïve T cells (T<sub>NAIVE</sub>: CCR7<sup>+</sup>CD45RO<sup>-</sup>), central memory (T<sub>CM</sub>: CCR7<sup>+</sup>CD45RO<sup>+</sup>), effector memory (T<sub>EM</sub>: CCR7<sup>-</sup>CD45RO<sup>+</sup>) and terminally differentiated effector T cells (T<sub>EMRA</sub>: CCR7<sup>-</sup>CD45RO<sup>-</sup>). (b) Strategy for defining T cell differentiation phenotypes applied to antigen-reactive CD4<sup>+</sup>CD137<sup>+</sup> and CD8<sup>+</sup>CD137<sup>+</sup> T cells after SpCas9 or human CMV<sub>pp65</sub> PBMCs stimulation. Summarized phenotypical distribution of (c) bulk un-stimulated, (d) SpCas9-reactive (CD137<sup>+</sup>) and (e) CMV<sub>pp65</sub>-reactive (CD137<sup>+</sup>) CD4<sup>+</sup> and CD8<sup>+</sup> T cells. Flow cytometric analysis of PBMCs from a representative donor. (SpCas9: n=24. CMV<sub>pp65</sub>: n=10. Horizontal line in graphs indicates median value.)



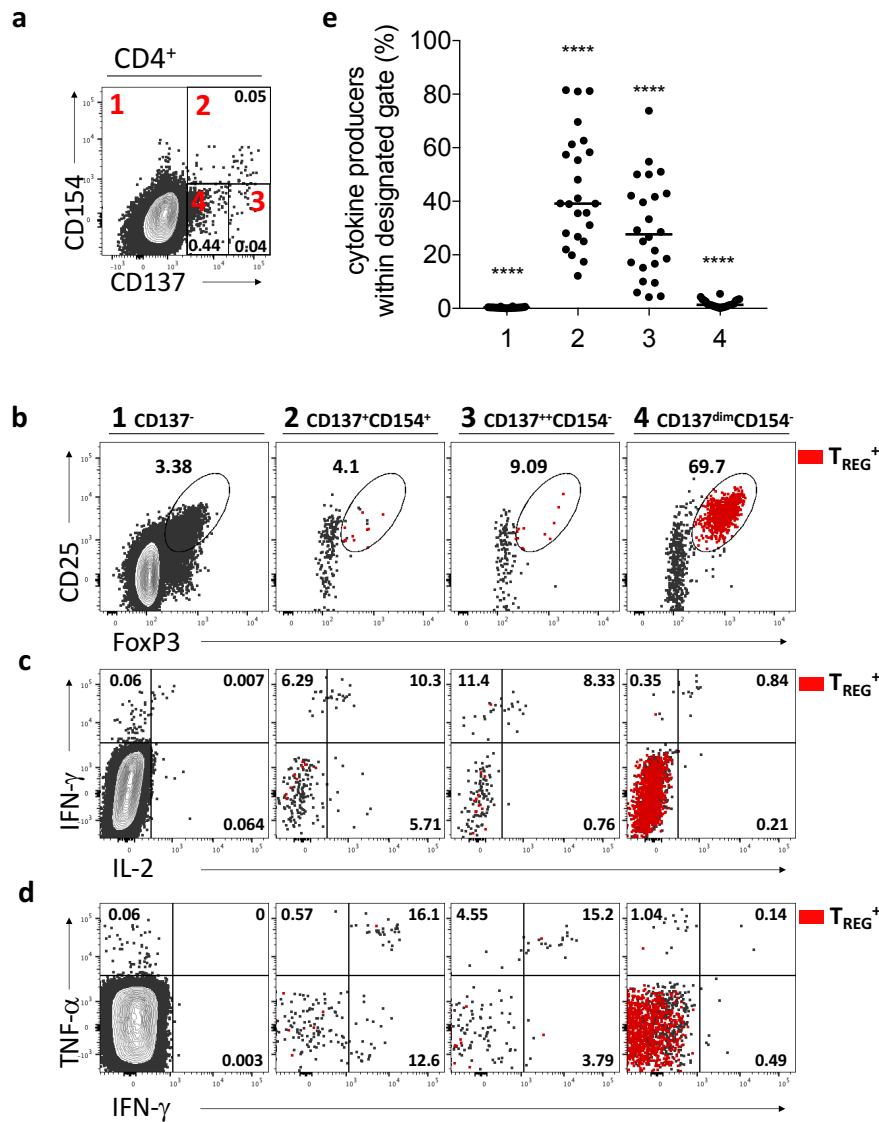
**Extended Data Figure 3. SpCas9-reactive CD4<sup>+</sup>CD137<sup>+</sup> regulatory T cells show a memory phenotypic profile.**

(a) Gating strategy for the identification of T<sub>REG</sub> phenotypes within the CD4<sup>+</sup> T cell response. (b) Summary of T<sub>REG</sub>-defining markers CD25, FoxP3, CTLA-4 and CD127 within SpCas9-activated CD4<sup>+</sup>CD137<sup>+</sup> and CD8<sup>+</sup>CD137<sup>+</sup> T cells. (c and d) Summary of T cell differentiation phenotypes within SpCas9-reactive CD4<sup>+</sup>CD137<sup>+</sup>FoxP3<sup>+</sup> T<sub>EFF</sub> and CD25<sup>+</sup>Foxp3<sup>+</sup> T<sub>REG</sub>. (n=24. Horizontal lines in graphs indicate median values.)



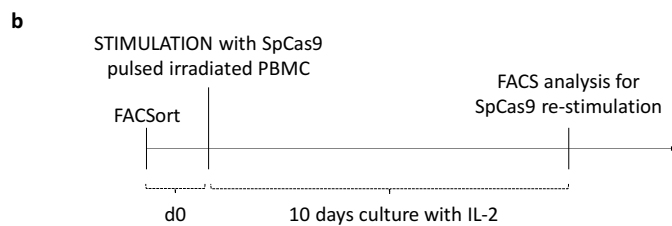
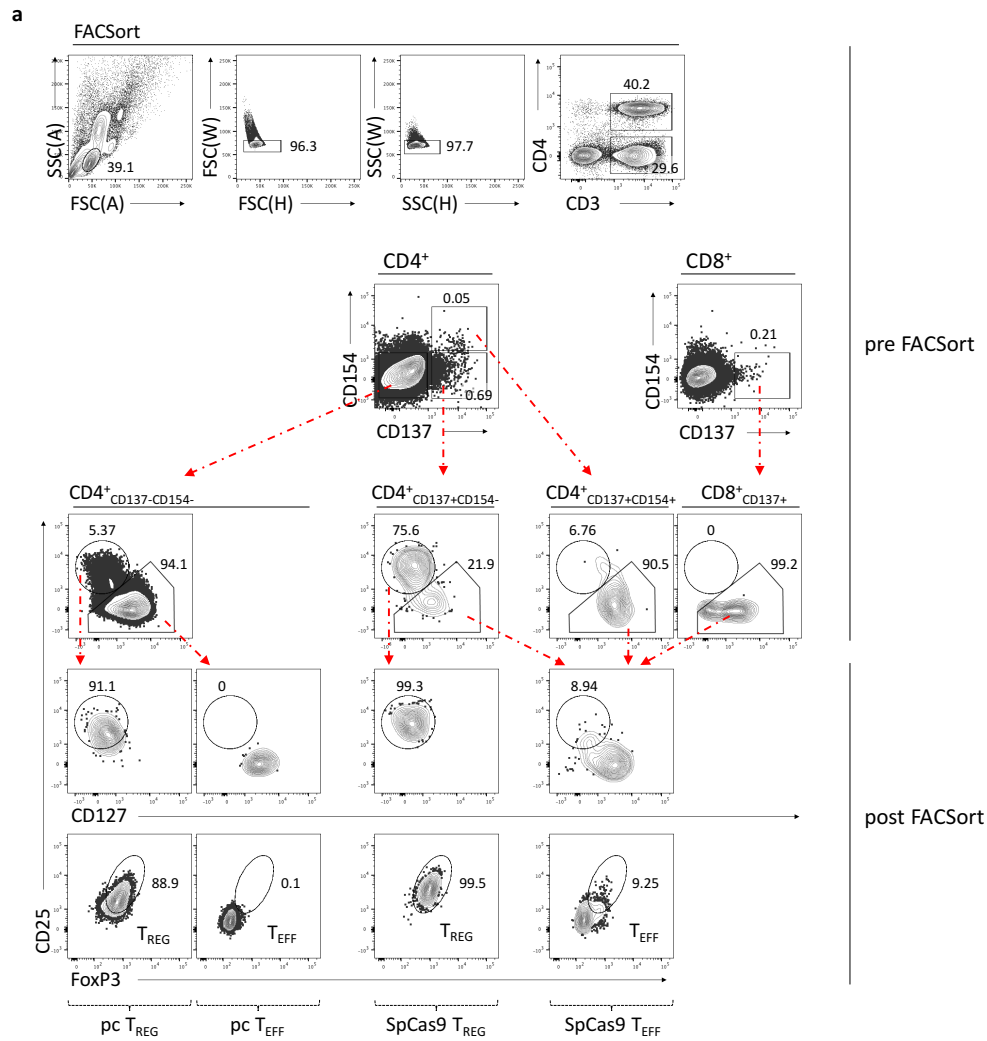
### Extended Data Figure 4. SpCas9-induced CD137 and CD154 expression correlate with lineage determining transcription factor pattern.

The SpCas9-induced activation pattern on CD4<sup>+</sup> was dissected according to CD137 and CD154 expression levels: (1): CD137<sup>-</sup>, (2) CD137<sup>+</sup>CD154<sup>+</sup>, (3) CD137<sup>high</sup>CD154<sup>-</sup> and (4) CD137<sup>dim</sup>CD154<sup>-</sup>. SpCas9-reactive CD8<sup>+</sup> T cells were defined through CD137 expression. Identification of Tbet (T<sub>EFF</sub>) and FoxP3 (T<sub>REG</sub>) transcription factors within (a) the CD4<sup>+</sup> T cell response (1 to 4) and (b) the CD8<sup>+</sup> T cell response to 16 h stimulation of human PBMCs with SpCas9 whole protein. (c and d) Summary of Tbet and FoxP3 expression within SpCas9-activated CD3<sup>+</sup> T cells with designated activation pattern (CD4<sup>+</sup>: 2 to 4; CD8<sup>+</sup>: CD137<sup>+</sup>). (n=6; horizontal lines within graphs indicate median values.)

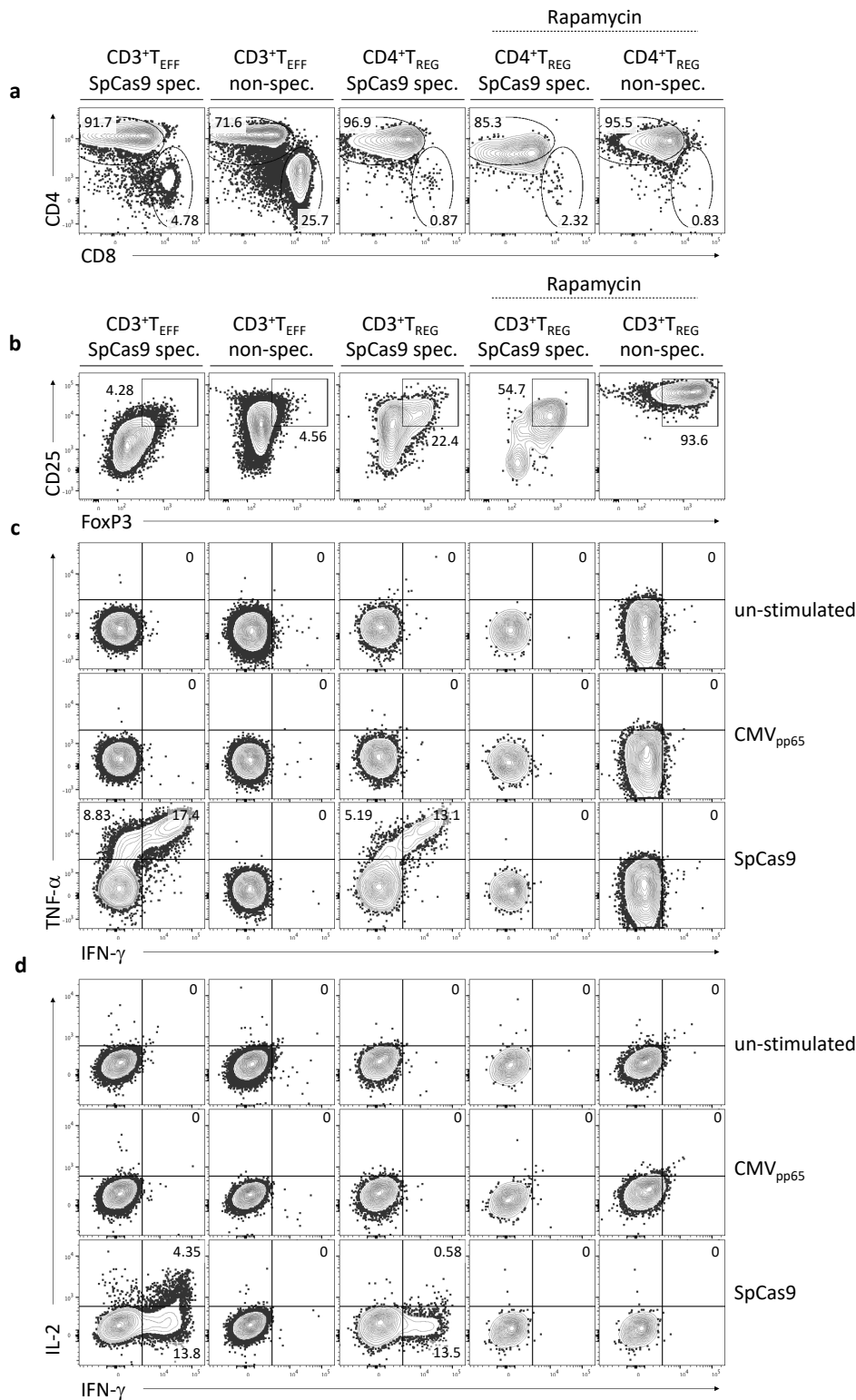


**Extended Data Figure 5. SpCas9-reactive CD4<sup>+</sup> regulatory T cells are CD137<sup>dim</sup> and lack CD154 expression and effector cytokine production.**

SpCas9-induced activation pattern on CD4<sup>+</sup> T cells was dissected according to CD137 and CD154 expression levels: (1): CD137<sup>-</sup>, (2) CD137<sup>+</sup>CD154<sup>+</sup>, (3) CD137<sup>high</sup>CD154<sup>-</sup> and (4) CD137<sup>dim</sup>CD154<sup>-</sup>. (a) Representative FACS plots for SpCas9-induced activation pattern (1-4) and corresponding (b) T<sub>REG</sub> phenotype (CD25<sup>+</sup>Foxp3<sup>+</sup>) and (c and d) effector cytokine production. Overlay demonstrates T<sub>REG</sub> contribution to the SpCas9-induced T cell response (red). (e) Summary of accumulated cytokine production within T cells with designated activation pattern (1 to 4).



**Extended Data Figure 6. Flow cytometric enrichment of SpCas9-reactive T<sub>EFF</sub> and T<sub>REG</sub>.** PBMCs were cultured for 16 h in the presence of 8  $\mu\text{g/ml}$  SpCas9 whole protein and 1  $\mu\text{g/ml}$  CD40-specific antibody. **(a)** SpCas9-specific T<sub>REG</sub>/T<sub>EFF</sub> and un-stimulated pc T<sub>REG</sub>/T<sub>EFF</sub> were enriched by FACS sorting according to the incremental gating of CD3<sup>+</sup>  $\rightarrow$  CD4<sup>+</sup> or CD8<sup>+</sup>  $\rightarrow$  CD137<sup>+/-</sup> CD154<sup>+/-</sup> or CD137<sup>+/-</sup>  $\rightarrow$  CD25<sup>high/low</sup> CD127<sup>+/-</sup>. Post-sorting purity is shown in lower panels for CD4<sup>+</sup>CD137<sup>-</sup>CD154<sup>-</sup>CD25<sup>high</sup>CD127<sup>-</sup> (pc T<sub>REG</sub>), CD4<sup>+</sup>CD137<sup>-</sup>CD154<sup>-</sup>CD25<sup>low</sup> and CD8<sup>+</sup>CD137<sup>-</sup>CD154<sup>-</sup>CD25<sup>low</sup> (pc T<sub>EFF</sub>), CD4<sup>+</sup>CD137<sup>+</sup>CD154<sup>-</sup>CD25<sup>high</sup>CD127<sup>-</sup> (SpCas9 T<sub>REG</sub>) and CD4<sup>+</sup>CD137<sup>+</sup>CD154<sup>+</sup>CD25<sup>low</sup>, CD4<sup>+</sup>CD137<sup>+</sup>CD154<sup>-</sup>CD25<sup>low</sup> and CD8<sup>+</sup>CD137<sup>+</sup> (SpCas9 T<sub>EFF</sub>). Representative flow cytometric images shown. (n=2). **(b)** Experimental design for expansion and re-stimulation of enriched SpCas9-reactive T<sub>EFF</sub> and SpCas9-reactive T<sub>REG</sub> and respective pc control populations.



### Extended Data Figure 7. Expansion of SpCas9-reactive T cells.

Antigen-specific readout for SpCas9-reactive *ex vivo* isolated and expanded T cells. Cultured SpCas9-specific T<sub>EFF</sub> and T<sub>REG</sub> were analysed at day 10 for expression of effector molecules in response to stimulation with SpCas9 whole protein loaded autologous moDCs for 6 h at a ratio of 10:1. Following stimulation, we analysed the expression of CD3, CD4, CD8, CD25, intracellular IFN- $\gamma$ , TNF- $\alpha$ , IL-2 and FoxP3. (a) CD4 to CD8 ratio, (b) CD25 and FoxP3 expression, (c) TNF- $\alpha$  and IFN- $\gamma$  and (d) IFN- $\gamma$  and IL-2 production within designated populations upon different stimuli (SpCas9, CMV<sub>pp65</sub> and control).